

## Influence of Lewis Base on the Nonstoichiometry and the Properties of Magnetite Films Prepared by Aqueous Solution Method

Don Kim,\* Kisoan Hwang, Chung Sub Lee,<sup>†</sup> Jung Chul Sur,<sup>‡</sup> Hyun Kwan Shim, and Yeong Il Kim

*Department of Chemistry, Pukyong National University, Pusan 608-737, Korea*

<sup>†</sup>*Department of Physics, Pukyong National University, Pusan 608-737, Korea*

<sup>‡</sup>*Department of Physics, Wonkwang University, Iksan 570-949, Korea*

*Received July 3, 1999*

Lewis bases were employed to control the stoichiometry of ferrite film prepared by light enhanced plating (LEP) technique. When 2,2'-bipyridyl was used as a Lewis base, conversion electron Mössbauer spectroscopy (CEMS) and x-ray powder diffraction (XRD) experiments showed that the main component of the ferrite films was metal-deficient magnetite ( $\text{Fe}_{3(1-\delta)}\text{O}_4$ ). Nonstoichiometry and roughness of LEP films were increased by the addition of 2,2'-bipyridyl. Using ethylenediaminetetraacetate (EDTA) as a Lewis base, produced film that was a mixture of magnetite and  $\gamma\text{-FeO}(\text{OH})$ . No low temperature transition (Verwey transition) of magnetite was detected in resistivity and ac-susceptibility measurements for the LEP films. Surface morphology of the LEP films was observed by atomic force microscopy (AFM). The size of dominant particles was about 0.2  $\mu\text{m}$ .

### Introduction

Light Enhanced Plating (LEP) process is a very good method for depositing magnetite films on various substrates from aqueous solutions at temperatures below the boiling point of water.<sup>1,2</sup> According to reports, LEP film has properties suitable for various applications: biosensors, chemical sensors, magnetic memory, artificial bioorgans, etc.<sup>1</sup> Physicochemical properties of magnetite strongly depend on the nonstoichiometric value ( $3\delta$ ) of  $\text{Fe}_{3(1-\delta)}\text{O}_4$ .<sup>2</sup> Therefore, controlling and determining the value of  $3\delta$  is important to understand the film's physicochemical properties, which determine potential applications. The  $3\delta$  implies a  $\text{Fe}^{2+}/\text{Fe}^{3+}$  ratio in the magnetite film. The  $\text{Fe}^{2+}/\text{Fe}^{3+}$  ratio of the reaction solution will greatly effect the ratio of the film. Therefore, we have tried to control the  $3\delta$  with the addition of complex-forming reagents - 2,2'-bipyridyl and EDTA - to the reaction solution. According to the formation constant table,<sup>3</sup> the former reagent prefers to form a complex with  $\text{Fe}^{2+}$ , but the latter reagent prefers to form a complex with  $\text{Fe}^{3+}$ . Hori *et al.*<sup>4</sup> have reported that the quality of LEP film surface improved with the addition of a small amount of Lewis base (0.01-0.04 g/L of dextran) to the LEP reaction solution. They also found that the  $\text{Fe}^{2+}/\text{Fe}^{3+}$  ratio in LEP film decreased with the addition.<sup>4</sup> However, they reported that their finding came from Fe-dextran complex.<sup>4</sup> Further investigation is needed to understand the role of Lewis bases, which prefer the special oxidation state of iron.

A Mössbauer experiment is an excellent non-destructive method to determine the ionic state and site occupation of Fe in iron compounds.<sup>5</sup> Because the normal Mössbauer spectrum represents  $\gamma$ -ray absorbance of Fe ions, the technique is useless if a film is deposited on a thick substrate.<sup>6</sup> In our previous work,<sup>2</sup> LEP film was collected in a powder from the glass substrate to obtain a normal Mössbauer spectrum. However, CEMS spectrum, which records scattered electron

energy, reveals surface characteristics of a film, regardless of the nature of the substrate.<sup>7</sup> Therefore, we used CEMS to obtain detailed ion distribution of an as-grown LEP film. The well known spectrophotometric method,<sup>8</sup> which needs more than 20 mg of sample to give reasonable results for the  $\text{Fe}^{2+}/\text{Fe}^{3+}$  ratio, was not applicable to our LEP films.<sup>2</sup>

In this work, we controlled the nonstoichiometry of the film with the addition of complex forming agents to the reaction solution of the LEP process. The distribution of Fe ions in LEP films was determined by CEMS, and the surface morphology of the film was observed by AFM. Electrical resistance and ac-susceptibility of LEP films were measured between 15 K and 295 K, confirming the existence of the low temperature transition (Verwey transition)<sup>9</sup> of magnetite and suggesting fine structure of LEP films.

### Experimental Section

**Film preparation.** The following is a brief description of LEP instrumentation and deposition condition of LEP films. See elsewhere for more details.<sup>2</sup> As the reaction solution flows through the gap between the glass substrate and stainless steel block with light radiation (Xe-lamp 300W), LEP ferrite film is deposited on a substrate. The flow rate of the reaction solution ( $\text{FeCl}_2$ , 3.0 g/L), which is 6 mL/min for 5 sec, and that of the oxidant solution ( $\text{NaNO}_2$ , 1.0 g/L) which is 11 mL/min for 0.5 sec, are controlled by two LC-pumps and a PC based controller for 7 minutes. A temperature controller and two cartridge heaters maintain the reaction temperature. The complex forming reagents (EDTA and 2,2'-bipyridyl) are added to the oxidant solution. The upper limit concentrations for a LEP deposition at 343 K were 2.0 g/L of 2,2'-bipyridyl and 0.25 g/L of EDTA. Above these concentrations no film was deposited.

**Characterization of LEP film.** AFM images of the films were observed by Autoprobe-PC (Park Scientific

Instruments) in contact mode with a commercially available cantilever ( $\text{Si}_3\text{N}_4$ ). The force constant of the cantilever is 0.05 N/m. The scan speed was less than 5 Hz. The structure of the film was identified with an X-ray diffractometer (Rikagu D/MAX2400) with  $\text{Cu-K}\alpha$  radiation. The lattice constant was calculated by extrapolation of Nelson-Riley fitting:<sup>10</sup>  $1/2(\cos^2\theta/\sin\theta + \cos^2\theta/\theta)$  vs. lattice constant. The patterns were compared with a stoichiometric magnetite sample<sup>2,11</sup> and joint committee for powder diffraction standards (JCPDS) data.<sup>12</sup> The CEMS spectrum was recorded at room temperature with an  $\text{He/CH}_4$  gas filled proportional counter and  $\text{Co}^{57}$  source doped in metallic rhodium, which is oscillated in a sinusoidal mode. The doppler velocity of the spectra was calibrated with  $\alpha\text{-Fe}$  foil (25  $\mu\text{m}$  in thickness). The resistivity of a sample was measured by 4-probe or 2-probe dc method using a nanovoltmeter (Keithley 182) and a current source (Keithley 224), or an electrometer (Keithley 617). Temperature of the sample was controlled by a closed cycle helium refrigerator (APD CSW-202) and a temperature controller (LakeShore M330). Ac-susceptibility measurement (dM/dH) was performed by an ac-susceptometer (LakeShore 7130). In the experiment, a magnetic field of 1.0 Oe was oscillated at a frequency of 125 Hz under a static zero field while the temperature was scanned from 13 K to 295 K. Magnetic susceptibility measurements ( $\chi_{\text{dc}}$  and  $\chi_{\text{ac}}$ ) for many magnetic materials yield the same result because  $\chi_{\text{dc}} = M/H$  is equal to  $\chi_{\text{ac}} = dM/dH$  for a well behaved paramagnet with zero field cool condition. LEP film was deposited on a polycarbonate film for the ac-susceptibility measurement.

## Results and Discussion

**AFM.** Figure 1 (a)-(d) show AFM images of 2,2'-bipyridyl

added LEP films deposited at 343 K, and Figure 1(e) shows the image of the film deposited at 363 K. The surface of the LEP films is packed with particles. Figure 1(a) and (b) are very close to the image of LEP films prepared without complex-forming agent.<sup>2</sup> The size of the dominant particles on the surface is about 0.2  $\mu\text{m}$  when the concentration of 2,2'-bipyridyl is less than 1.0 g/L. The particle size is close to that of the powders prepared by other wet chemical methods.<sup>13,14</sup> When the concentration of 2,2'-bipyridyl is  $>1.0$  g/L, the particle size is increased and the roughness of film surface is also increased. A few large particles, those about 0.7  $\mu\text{m}$  in diameter, are found at the highest limit concentration of 2,2'-bipyridyl used here, as shown in Figure 1(d). Above that concentration, magnetite is not deposited on the substrate because most  $\text{Fe}^{2+}$  ions are removed by the excess Lewis base. The size of the dominant particles is independent of the reaction temperature of the LEP process. The surface was also observed by scanning electron microscopy (SEM). The spherical particles of a LEP film surface were identified as granular particles in the SEM picture. But, we could not observe the fine structure of the particles by AFM because the apparent diameter of protrusions rendered with AFM contains a contribution of the geometry of the AFM probe tip.<sup>15</sup> The pyramidal-shaped particles in Figure 1(e) were clearly observed in the SEM picture.<sup>16</sup> When EDTA was added to the LEP process, the surface morphology and the particle size ( $\sim 0.2$   $\mu\text{m}$ ) of the film are very similar to those of normal LEP film deposited without Lewis base. But the surface was rougher than that of normal LEP film.

**XRD.** XRD patterns of the 2,2'-bipyridyl added LEP films are shown in Figure 2. These patterns matched well with JCPDS data of magnetite (99.99%)<sup>12,13</sup> and stoichiometric synthetic magnetite sample (99.999%)<sup>2,11</sup> as shown in Figure 2. There is no peak broadening caused by fine parti-

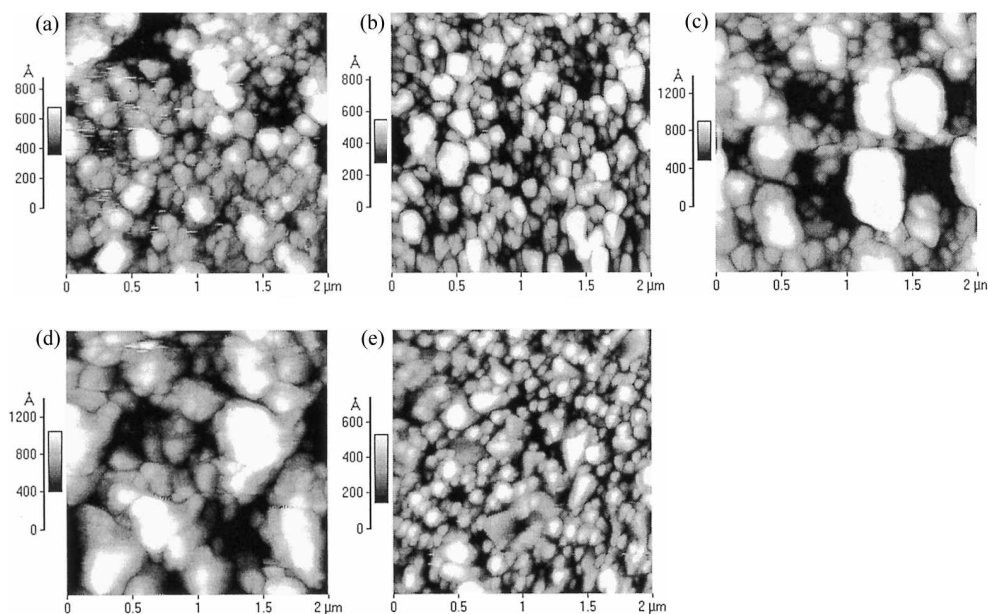


**Figure 1.** AFM images of LEP films. Concentrations of 2,2'-bipyridyl in the oxidation solution were (a) 0.02 g/L, (b) 0.50 g/L, (c) 1.650 g/L, (d) 2.00 g/L, at 343 K. And (e) was deposited at 363 K with 1.00 g/L of 2,2'-bipyridyl.

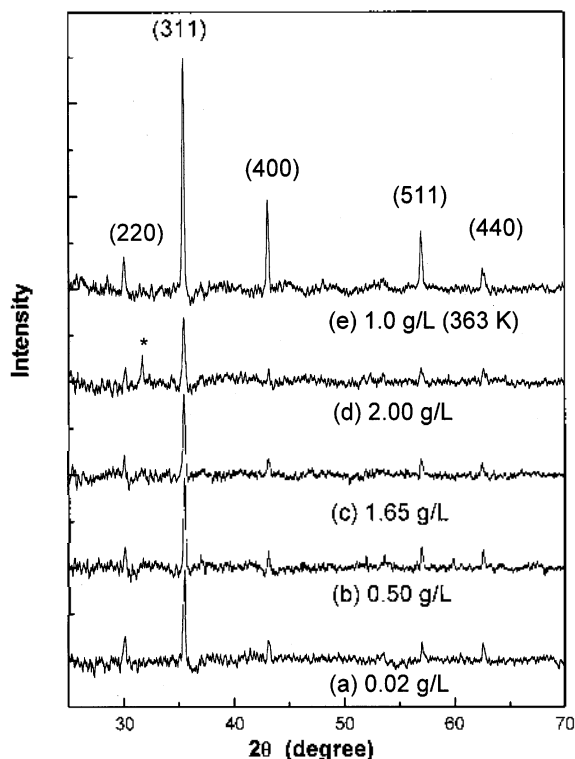


**Figure 2.** XRD pattern of LEP films. The films were deposited at 343 K. concentrations of 2,2'-bipyridyl in the oxidation solution were (a) 0.02 g/L, (b) 0.50 g/L, (c) 1.65 g/L, (d) 2.00 g/L. And (e) was deposited at 363 K with 1.00 g/L of 2,2'-bipyridyl.

cles. But there is a strange reflection(\*) that does not match the magnetite peaks in Figure 2(d). According to the JCPDS data, no other iron compound formed by the LEP process has a reflection plane at the position ( $2\theta = 32.08^\circ$ ), except (011) reflection of  $\gamma$ -FeO(OH).<sup>12,13</sup> However, we do not have additional experimental evidences to confirm the  $\gamma$ -FeO(OH) phase.

During the LEP reaction, 2,2'-bipyridyl does not form a complex with  $\text{Fe}^{3+}$  but with  $\text{Fe}^{2+}$ . Consequently, the concentration of  $\text{Fe}^{2+}$  will decrease by the addition of 2,2'-bipyridyl to the reaction solution and the more nonstoichiometric magnetite phase will be deposited on the substrate. According to the report by Tamaura *et al.*,<sup>17</sup> the lattice parameter of polycrystalline magnetite decreases along with nonstoichiometry:  $a_0 = 0.8418$  nm for  $3\delta = -0.127$ ,  $a_0 = 0.83967$  nm for  $3\delta = 0.000$ ,  $a_0 = 0.8394$  nm for  $3\delta = 0.017$ ,  $a_0 = 0.8389$  nm for  $3\delta = 0.113$ . this explanation can be proved qualitatively by the comparison of lattice parameters of LEP films. Lattice parameters ( $a_0$ ) of LEP films were estimated by the extrapolation of Nelson-Riley fitting,<sup>10</sup> as listed in Table 1. The estimated lattice parameters (fitting error  $\pm 0.00005$  nm) are not far from those of the JCPDS ( $a = 0.83967$  nm)<sup>12</sup> and the "no Lewis base added" LEP film ( $a = 0.8395$  nm). The lattice parameters decrease roughly with the addition of 2,2'-bipyridyl. Even though the dependency of the lattice parameters on the concentration of 2,2'-bipyridyl is somewhat unclear, the trend indicates that  $3\delta$  of the magnetite phase increases with the addition of 2,2'-bipyridyl, which plays the

**Table 1.** Lattice parameters and chemical formulas of 2,2'-bipyridyl added LEP films. All LEP films was deposited at 343 K except one sample. Area ratio ( $I_{011}/I_{T1}$ ) and chemical formula were estimated by Mössbauer spectra

Concentration of 2,2'-bipyridyl (g/L)	Lattice parameter (nm)	$I_{011}/I_{T1}$	Chemical Formula
0.02	0.83961	1.54	$(\text{Fe}^{3+}_{1.00})[\text{Fe}^{3+}_{0.18}(\text{Fe})_{1.82}]\text{O}_4$
0.50	0.83930	1.49	$(\text{Fe}^{3+}_{1.00})[\text{Fe}^{3+}_{0.21}(\text{Fe})_{1.80}]\text{O}_4$
1.65	0.83915	1.28	$(\text{Fe}^{3+}_{1.00})[\text{Fe}^{3+}_{0.32}(\text{Fe})_{1.68}]\text{O}_4$
2.00	0.83907	0.89	$(\text{Fe}^{3+}_{1.00})[\text{Fe}^{3+}_{0.50}(\text{Fe})_{1.41}]\text{O}_4$
1.00(363K)	0.83967	1.65	$(\text{Fe}^{3+}_{1.00})[\text{Fe}^{3+}_{0.13}(\text{Fe})_{1.87}]\text{O}_4$

same role as an oxidizing agent. Quantitative analysis of the trend will be discussed in the Mössbauer section.

EDTA, which prefers to form  $\text{Fe}^{3+}$  - EDTA complex, was used to increase  $\text{Fe}^{2+}/\text{Fe}^{3+}$  ratio of the reaction solution. As shown in Figure 3, all XRD patterns of LEP films deposited from EDTA containing solution have main reflections of magnetite. When more than 0.02 g/L of EDTA were added to the LEP solution at 343K,  $\gamma$ -FeO(OH) phase appeared. The arrows in Figure 3 indicate reflections of the  $\gamma$ -FeO(OH). When the LEP film was exposed to ambient air immediately after deposition the color of LEP film changed from black to dark brown within 1 minute. From the color change, we concluded the  $\gamma$ -FeO(OH) is the result of the air oxidation of  $\text{Fe}^{2+}$  ions on the surface of LEP film. Also FeO(OH) is one possible intermediate of the dissolution process of

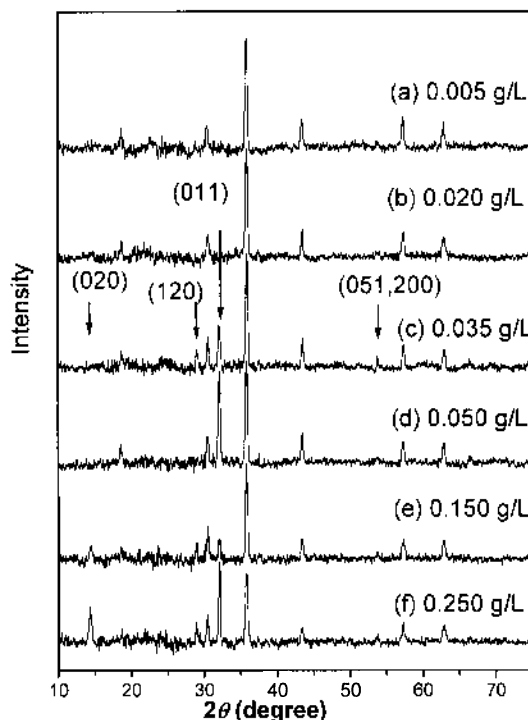


**Figure 3.** XRD patterns of EDTA added LEP films. The films were deposited at 343 K. Arrows indicate reflection positions of  $\gamma$ -FeO(OH). Other peaks are matched well with XRD pattern of magnetite.

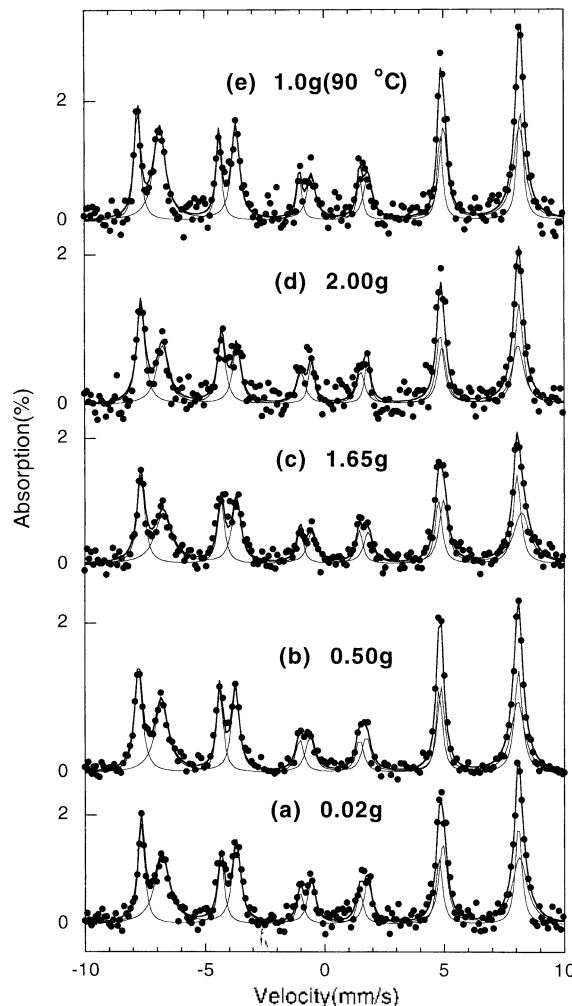
**Table 2.** Lattice parameters of EDTA added LEP films. Films were deposited at 343 K

Concentration of EDTA(g / L)	Lattice Parameter (nm)
0.005	0.83967
0.020	0.83957
0.035	0.83960
0.050	0.83961
0.150	0.83951
0.250	0.83967

magnetite in the EDTA containing solution.<sup>18</sup> More careful work is needed to understand the effects of EDTA in the LEP process. Lattice parameter (fitting error  $\pm 0.00005$  nm) of the magnetite phase in the EDTA-added LEP films was evaluated by the Nelson-Riley function. As shown in Table 2, lattice parameters of EDTA-added films are very close to those of magnetite in JCPDS data, and they are independent of the concentration of EDTA. This indicates that  $3\delta$  of the magnetite phases is close to zero. Therefore, we assume the magnetite phase is stoichiometric magnetite. The stoichiometric magnetite phase may be deposited because excess  $\text{Fe}^{3+}$  ions are removed by EDTA- $\text{Fe}^{3+}$  complex formation during the LEP process.

**CEMS.** The Mössbauer spectrum of the magnetite is magnetically split.<sup>5</sup> Figure 4 shows that CEMS spectra of LEP films is very similar to that of magnetite.<sup>2,5</sup> This indicates LEP films are not in superparamagnetic state at room temperature. A difference between CEMS spectrum and normal Mössbauer spectrum is reversed peak direction in spectrum, because normal Mössbauer spectrum is a record of  $\gamma$ -ray absorption and CEMS spectrum is a record of scattered signal. Therefore the CEMS spectrum can be deconvoluted by a standard fitting method with reversed intensity of spectrum. The deconvolution is described in detail elsewhere.<sup>2</sup> In Figure 4, CEMS spectra of LEP films could be deconvoluted to two sextets marked by  $T_d$  and  $O_h$ . The set of  $T_d$  results from tetrahedral(A) sites and the set of  $O_h$  results from octahedral(B) sites of  $(\text{Fe}^{3+})_A(\text{Fe}^{2+}\text{Fe}^{3+})_B\text{O}_4$ , where ( ) denotes A site and [ ] denotes B site. In Table 1, the area ratio ( $I_{O_h}/I_{T_d}$ ) of peaks corresponds to the population ratio of Fe ions in octahedral sites and tetrahedral sites.

Mössbauer parameters for LEP films were close to those of the reported value of magnetite:<sup>5</sup> isomer shifts for A site and B site are about 0.28 mm/s and 0.68 mm/s, and corresponding magnetic hyperfine fields are about 490 kOe and 460 kOe, respectively. This result indicates that some  $\text{Fe}^{3+}$  in B sites are not involved in the hopping process between  $\text{Fe}^{2+}$  and  $\text{Fe}^{3+}$  in B sites of inverse spinel structure of magnetite. This extra  $\text{Fe}^{3+}$  in B sites contributes to the sextet of  $T_d$  in Mössbauer spectrum.<sup>5</sup> The formation of the extra  $\text{Fe}^{3+}$  in B sites was reported in ferrite solid solutions and epitaxial thin film of magnetite.<sup>5</sup> In these systems, sextet of  $T_d$  is due to the contribution of  $\text{Fe}^{3+}$  in both A and B sites, and sextet of  $O_h$  is due to the contribution of electron exchange between  $\text{Fe}^{2+}$  and  $\text{Fe}^{3+}$  in the B sites, forming average valence  $\text{Fe}^{2.51}$ .<sup>5(c)</sup>

**Figure 4.** Room temperature CEMS spectra of LEP films which were prepared at various concentrations of 2,2'-bipyridyl.  $T_d$  indicates tetrahedral site and  $O_h$  indicates octahedral site. The deposition temperature is 343 K, if not indicated.

Therefore, we could estimate the cation distribution of LEP film from the  $I_{O_h}/I_{T_d}$  (fitting error  $\pm 0.05$ ) of LEP film as listed in Table 1. The chemical formula in Table 1 is written to emphasize the presence of special  $\text{Fe}^{3+}$ , which does not take part in the exchange process at octahedral sites. The formula implies  $(\text{Fe}^{3+})_A[\text{Fe}^{3+}_{1.5\delta}(\text{Fe}^{3+}_{1-9\delta}\text{Fe}^{2+}_{1.9\delta})]_B\text{O}_4$ . That is the very same general formula of magnetite,  $\text{Fe}_{3(1-\delta)}\text{O}_4$ . From Table 1, it is clear that the amount of the nonstoichiometry ( $3\delta$ ) increases with the addition of 2,2'-bipyridyl, as expected. And the reaction temperature is another important factor for the control of the nonstoichiometry, because higher reaction temperature lead to more stoichiometric phase.

At room temperature Mössbauer parameters of  $\gamma\text{-FeO}$  (OII) are as follows: isomer shift is 0.37 mm/sec, quadrupole splitting is 0.52 mm/sec and no hyperfine field.<sup>13</sup> Therefore,  $\gamma\text{-FeO}$ (OII) will have doublet peaks near zero velocity at room temperature. The signal near the center of CEMS spectrum of EDTA-added LEP films was not clear due to base line noise; therefore, we could not obtain reasonable CEMS data on the films.

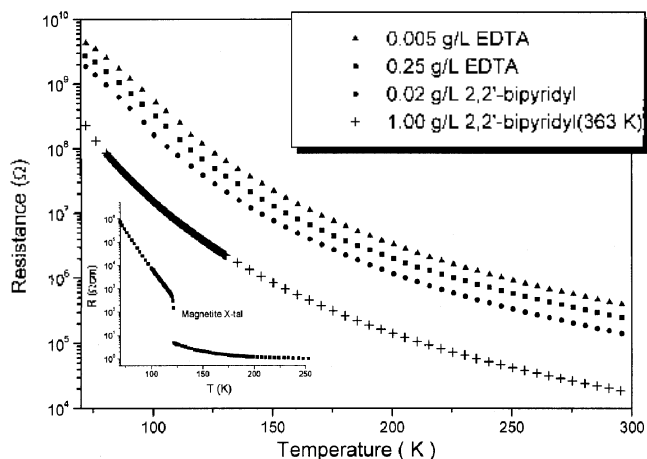


**Figure 5.** Plot of temperature vs. resistance of LEP films which were prepared at various concentration of Lewis bases. The deposition temperature is 343 K, except one ( $\cdot$ ). The inset shows Verwey transition of stoichiometric magnetite at about 120 K.

**Transport property.** According to the reports of Honig *et al.*, Verwey transition temperature ( $T_V$ ) of magnetite crystal,  $\text{Fe}_{1-(3\delta)}\text{O}_4$ , depends on the  $3\delta$  of magnetite in various physical property measurements:<sup>9,19</sup>  $T_V \sim 120$  K for  $3\delta = 0$ ,  $\sim 83$  K for  $3\delta = 0.039$ , and no transition for  $3\delta > 0.039$ . Figure 5 is the plot of resistance vs. temperature for a few Lewis base added LEP films. The inset of Figure 5 shows a breakpoint on resistivity vs. temperature curve. The sudden change is related to  $T_V$  of stoichiometric magnetite. In Figure 5, the  $3\delta$  of samples, which, estimated by Mössbauer experiment, are 0.026 for  $+$  and 0.034 for  $\bullet$ . The  $3\delta$  of EDTA-added samples is very close to ideal magnetite as discussed above. Therefore, a sudden change of slope ( $dR/dT$ ) is expected on the resistivity( $R$ ) vs. temperature( $T$ ) plot if the electrical conduction process of LEP films is the same as that of magnetite crystal. In Figure 5, the temperature dependence of resistivity is quite different from our previous report.<sup>2</sup> All the LEP films have nearly the same temperature dependency, and Verwey transition is not observed within the experimental temperature range. This indicates that the electrical transport characteristics of LEP films may not depend on the estimated  $3\delta$ . One possible explanation is that the nonstoichiometry of the electrical conduction path in a LEP film may be greater than 0.039, although the estimated  $3\delta$  is less than 0.039 from Mössbauer. Because the surface of magnetite nanoparticles is easily oxidized by the ambient air at room temperature, all nanoparticles in LEP films are covered by the highly nonstoichiometric magnetite phase that is highly resistive. For EDTA-added LEP films,  $\gamma\text{-FeO(OH)}$  phase also acts as a resistive phase, with the electrical contact between particles and the electrical conduction process depending on the highly resistive phase. Therefore, all LEP films show nearly same transport behavior in Figure 5. The possibility of the presence of the nanoparticles in LEP films is discussed in the following section.

**Ac-susceptibility.** Even though we have discussed the compositional inhomogeneous of LEP films, it is hard to

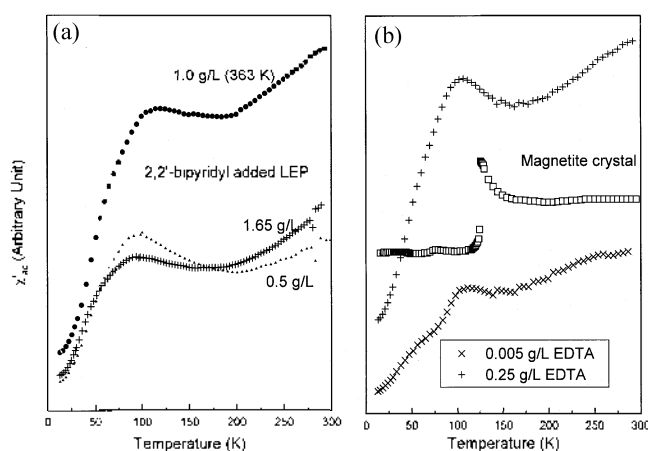


**Figure 6.** Real component ( $\chi'$ ) of ac-susceptibility was measured from 13 K to 295 K; (a) 2,2'-bipyridyl added LEP films. (b) magnetite single crystal and EDTA added LEP films. The most and the least nonstoichiometric LEP films are chosen for comparison in both plots.

find experimental evidence of this state in a magnetite crystal and a LEP film by resistivity and Mössbauer measurements. Highly sensitive ac-susceptibility measurements ( $2 \times 10^{-8}$  emu) are suitable to reveal such inhomogeneous in a magnetite crystal because the susceptibility signal reflects each partial component of the inhomogeneous phases, as reported by Aragon.<sup>20</sup> Ac-susceptibilities of Lewis base added LEP films and magnetite single crystal ( $3\delta = 0$ ) are compared in Figure 6. There is a sudden change on the curve for the stoichiometric magnetite crystal around 120 K. The change is related with Verwey transition of magnetite. Initially we expected that if  $3\delta$  of some part of a LEP films were less than 0.039, ac-susceptibility would be changed abnormally at the corresponding temperature of the nonstoichiometry of the phase, as observed in magnetite crystal. But all LEP films show a hump on the plot at around 100 K instead of a clear transition. This suggests that the magnetite particles on LEP film exhibit specific behaviors on the susceptibility vs. temperature curve.

Magnetic particles of very small size are known to mimic some of the properties of spin glass materials and to exhibit blocking temperature ( $T_B$ ).<sup>21</sup> Above  $T_B$  the particles are in the superparamagnetic state and below  $T_B$  the superparamagnetic behavior is blocked.<sup>22,23</sup> Therefore, there is splitting between field cooled and zero field cooled dc-susceptibility.<sup>23</sup> The splitting point is  $T_B$ .<sup>21</sup> Because the splitting emerges at around the hump on a plot of temperature vs. zero field cooled dc-susceptibility (or ac-susceptibility), we can estimate the  $T_B$  from the ac-susceptibility curve. Qualitatively the smaller particle, which easily rotates along with the magnetic field, has lower  $T_B$  and roughly obey the relationship  $T_B = K \cdot V / (30 \cdot k_B)$ , where  $K$  is anisotropy constant,  $V$  is the average volume of the particle and  $k_B$  is the Boltzmann's constant.<sup>24</sup>

In the Figure 6, all LEP films have a hump at about 100 K. The estimated particle size by the above relationship is 4.4 nm. This suggests that some of the LEP particles observed

by AFM are aggregated magnetite nanoparticles with a diameter of about 4.4 nm. Above the blocking temperature, however, LEP films show susceptibility behavior different from that of narrow-size-distributed magnetite nanoparticles<sup>22</sup> and magnetite crystal. The difference indicates the presence of various sizes of magnetite nanoparticles in the LEP films. If a great part of a LEP film is in the superparamagnetic state above 100 K, a distinctive doublet peak appears near the center of the CEMS spectrum recorded at room temperature. Also peak broadening will be observed in the XRD pattern. However, neither phenomena are observed in experiments. This implies that the number of nanoparticles, those that are superparamagnetic state at room temperature, is less than the detection limit of CEMS and XRD experiments. Nanoparticles in superparamagnetic state at room temperature are minor components of LEP films. According to a recent report by Makoto *et al.*,<sup>23</sup> stoichiometric magnetite clusters, ~50 nm in diameter and isolated in a glass matrix to avoid the superparamagnetic behavior and air oxidation, did not show an abnormal change of susceptibility at the temperature of Verwey transition. This indicates that strong magnetic interaction between magnetite fine particles is very important to reveal the Verwey transition in susceptibility measurements. The magnetite particles in LEP films will not have the strong interactions because of highly oxidized nanoparticles, therefore Verwey transition is not observed in Figure 6 even though the estimated  $3\delta$  of LEP films is less than 0.039.

### Conclusions

We have tried to control the nonstoichiometry of LEP ferrite films deposited from aqueous solutions by the addition of a couple of Lewis bases. When 2,2'-bipyridyl was added to the LEP process, basically metal deficient magnetite ( $\text{Fe}_{3(1-\delta)}\text{O}_4$ ) film was deposited on a substrate. According to XRD and CEMS studies, the nonstoichiometry ( $3\delta$ ) of the LEP film depends on the concentration of 2,2'-bipyridyl, which could form a complex only with  $\text{Fe}^{2+}$ . When EDTA was used as a Lewis base, the deposited film was a mixture of magnetite and  $\gamma\text{-FeO}(\text{OH})$ . The  $\gamma\text{-FeO}(\text{OH})$  results from the air oxidation of  $\text{Fe}^{2+}$  ions. Further work is needed to investigate this result.

**Acknowledgment.** We wish to thank Prof. J. M. Honig (Purdue Univ. Chem. Dept.) for his useful advice. This work was supported by the Korean Ministry of Education through Research Fund (BSRI-97-2455) and by Pukyong National University (1998).

### References

- (a) Abe, M.; Tamaura, Y. *Jpn. J. Appl. Phys.* **1983**, *22*, L511. (b) Abe, M.; Tanno, Y.; Tamaura, Y. *J. Appl. Phys.* **1985**, *57*, 3795. (c) Itoh, T.; Hori, S.; Abe, M.; Tamaura, Y. *IEEE Trans. Mag. Jpn.* **1991**, *6*, 214. (d) Abe, M.; Itoh, T.; Tamaura, Y. *Thin Solid Films* **1992**, *216*, 155. (e) Abe, M.; Itoh, T.; Zhang, Q. *Trans. Mat. Res. Soc. Jpn.* **1994**, *15B*, 1117. (f) Zhang, Q.; Itoh, T.; Abe, M. *J. Appl. Phys.* **1994**, *75*, 7171.
- Kim, D.; Lee, C. S.; Kim, Y. I. *Bull. Korean Chem. Soc.* **1998**, *19*, 533.
- Harris, D. C. *Quantitative Chemical Analysis*, 4th ed.; W.H. Freeman and Company, N.Y., 1995.
- (a) Hori, S.; Itoh, T.; Abe, M.; Tamaura, A. *IEEE Trans. Mag. Jpn.* **1992**, *7*, 290. (b) Lee, J. S.; Itoh, T.; Abe, M. *J. Kor. Phys. Soc.* **1995**, *28*, 375.
- (a) Haley, G.; Mullen, J. G.; Honig, J. M. *Solid State Comm.* **1989**, *6*, 285. (b) Kodama, T.; Tabata, M.; Sano, T.; Tsuji, M.; Tamaura, Y. *J. Solid State Chem.* **1995**, *120*, 64. (c) Voogt, F. C.; Hlibma, T.; Zhang, G. L.; Hoefman, M.; Niesen, L. *Surface Sci.* **1995**, 331-333, 1508.
- Vertes, A.; Korecz, L.; Burger, K. *Mössbauer Spectroscopy*; Elsevier: Budapest, 1979.
- Voogt, F. C.; Fujii, T.; Hlibma, T.; Hoefman, M.; Smulders, P. J. M.; Wijnja, F. H.; Zhang, G. L.; Niesen, L. *Hyperfine Interaction* **1996**, 97-98, 99.
- Iwasaki, I.; Katsura, T.; Ozawa, T.; Yoshida, M.; Mashima, M.; Haramura, H.; Iwasaki, B. *Bull. Volc. Soc. Jpn. Ser. II* **1960**, *5*, 9.
- Honig, J. M. *J. Alloy and Compounds* **1995**, 229, 24, and references therein.
- Azaroff, L. B. *The Powder Method*; McGraw Hill: New York, N.Y. 1958; p 238.
- Kim, D. KOSEF report (1997).
- JCPDS (Joint Committee on Powder Diffraction Standards) data base 19-629.
- Cornell, R. M.; Schwertmann, U. *The Iron Oxides*; VCH: Weinheim, Germany, 1996.
- Yuan, C.; Yang, X.; Fu, D.; Lu, Z.; Liu, J.; Zhang, C.; Wu, T.; Wang, L.; Peng, S. *J. Solid State Chem.* **1996**, *121*, 492.
- Hisao, G. S.; Anderson, M. G.; Gorer, S.; Harris, D.; Penner, R. M. *J. Am. Chem. Soc.* **1997**, *119*, 1439.
- Kim, D.; Park, J. C. Manuscript in preparation.
- Tamura, Y.; Tabata, M. *Nature* **1990**, *346*, 255.
- Tamura, H.; Takasaki, S. I.; Furuichi, R. *Bunseki Kagaku* **1998**, *47*, 397.
- (a) Kim, D.; Honig, J. M. *Phys. Rev. B* **1994**, *49*, 4438. (b) Kozłowski, A.; Kakol, Z.; Kim, D.; Zalecki, R.; Honig, J. M. *Phys. Rev. B* **1996**, *54*, 12093. (c) Kozłowski, A.; Kakol, Z.; Kim, D.; Zalecki, R.; Honig, J. M. *Z. Anorg. All. Chem.* **1997**, *623*, 115.
- Aragon, R.; Buttery, D. J.; Shepherd, J. P.; Honig, J. M. *Phys. Rev. B* **1985**, *31*, 430.
- Kommarreddi, N. S.; Tata, M.; John, V. T.; McPherson, G. L.; Herman, M. F.; Lee, T. S.; O'Conner, C. J.; Akkara, J. A.; Kaplan, D. L.; *Chem. Mater.* **1996**, *8*, 801.
- (a) Perez, J. A. L.; Mira, J.; Rivas, J.; Charles, S. W. *Phys. Chem. B* **1997**, *101*, 8045. (b) Kim, Y. I.; Kang, H. J.; Lee, C. S.; Kim, D. Manuscript in preparation.
- Rado, G. T.; Suhl, H. *Magnetism*; Academic: New York, 1963.
- Yamamoto, Y.; Hara, K. *IEEE Trans. Mag.* **1992**, *28*, 2365.
- Hagiwara, M.; Nagata, K.; Nagata, K. *J. Phys. Soc. Jpn.* **1998**, *67*, 3590.